

# **Force-Dependent Folding and Unfolding Kinetics in DNA Hairpins Reveals Transition State Displacements along a Single Pathway**

A. Alemany<sup>†</sup> and F. Ritort<sup>\*,†,‡</sup>

<sup>†</sup>*Small Biosystems Lab, Condensed Matter Physics Department, Universitat de Barcelona,  
Diagonal 647, 080028 Barcelona, Spain*

<sup>‡</sup>*Ciber-BBN, Networking Research Center of Bioengineering, Biomaterials and  
Nanomedicine, Instituto Carlos III, 28029 Madrid, Spain*

E-mail: ritort@ub.edu

# Supplementary Sections

## S1. Kinetic rates from equilibrium force-jump experiments

For the three hairpins HN, HC and HB it is extremely difficult to observe transitions between the unfolded and folded states within reasonable experimental timescales even when pulled at the coexistence force. In fact the height of the kinetic barrier is too large and thermal fluctuations not strong enough to induce the stochastic folding/unfolding of the hairpin in reasonable timescales (e.g. within a few seconds). Consequently, in order to obtain the force-dependent kinetic rates from equilibrium experiments we perform force jump experiments (Fig. 1). To determine the unfolding (folding) kinetic rate in these experiments at a force  $f$ , the hairpin was repeatedly and manually set to the folded (unfolded) states at force  $f$  waiting until a transition to the unfolded (folded) state was observed. The unfolding(folding) kinetic rate is then estimated as the inverse of the average lifetime of the folded(unfolded) state at that force.

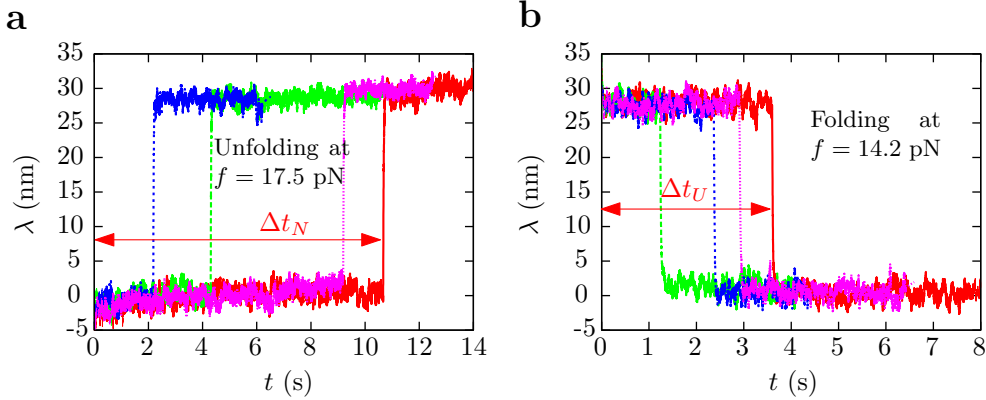


Figure 1: **Force-jump experiments.** Results for hairpin HN. **a.** Unfolding force-jump experiments carried out at 17.5 pN. **b.** Folding force-jump experiments carried out at 14.2 pN. Different repetitions in each case are shown.

As shown in Figure 2, kinetic rates estimated using this approach and pulling experiments give identical results, which validates the effective barrier approach for both equilibrium and non-equilibrium data. Therefore, the analysis presented here to extract  $B(f)$  is independent of the non-equilibrium or equilibrium origin of the experimental approach used to determine

the kinetic rates.

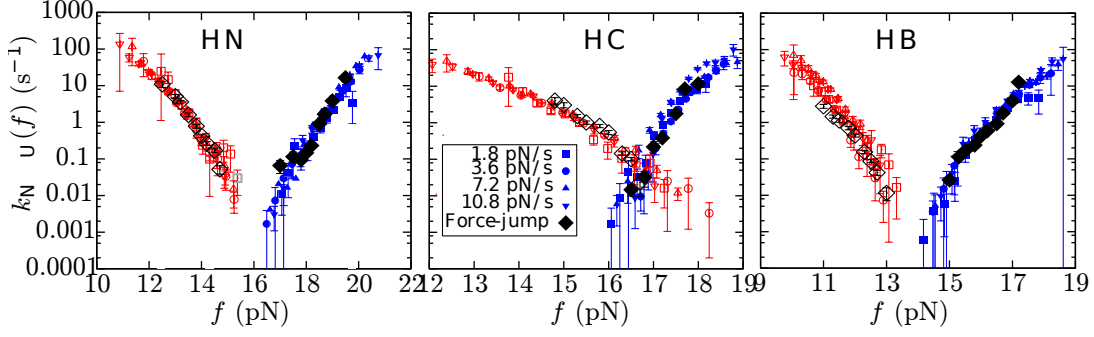


Figure 2: **Kinetic rates for hairpins HN, HC and HB.** Kinetic rates of unfolding (blue-solid symbols) and folding (red-empty symbols) measured from pulling experiments performed at different loading rates and force-jump experiments (black symbols) for the three hairpins HN, HC and HB.

## S2. Kinetic rates in the Bell-Evans model

According to the Bell-Evans (BE) model, the unfolding and folding kinetic rates read as:

$$k_{\text{unf}}(f) = k_0 \exp\left(-\frac{B - fx_F^\dagger}{k_B T}\right) = k_m \exp\left(\frac{fx_F^\dagger}{k_B T}\right) \quad (1)$$

$$k_{\text{fold}}(f) = k_0 \exp\left(-\frac{B - \Delta G_{NU} + fx_U^\dagger}{k_B T}\right) = k_m \exp\left(\frac{\Delta G_{NU} - fx_U^\dagger}{k_B T}\right), \quad (2)$$

where  $B$  is the kinetic barrier;  $k_m = k_0 \exp(-B/k_B T)$  is the unfolding kinetic rate at zero force;  $x_F^\dagger = x_{\text{TS}} - x_F$  and  $x_U^\dagger = x_U - x_{\text{TS}}$  are the relative distances between states  $U$  and  $F$  with respect to the TS at the coexistence force  $f_c$ , respectively. Their sum should be equal to the molecular extension  $x_N = x_U - x_F = x_F^\dagger + x_U^\dagger$ ; and  $\Delta G_{NU} = f_c x_N$  is related to the free-energy difference between states  $F$  and  $U$ . Note that  $k_{\text{fold}}(f_c) = k_{\text{unf}}(f_c)$ .

The experimentally measured  $k_{\text{unf}}(f)$  and  $k_{\text{fold}}(f)$  for hairpins HN, HC and HB are first fitted to Eqs. (1) and (2) along the entire experimentally available range of forces in order to extract  $k_m$ ,  $\Delta G_{NU}$ ,  $x_F^\dagger$ ,  $x_U^\dagger$  and  $f_c$ . Results of such linear fits (in a  $\log(k)$  versus  $f$  representation) for the three hairpins are shown in Fig. 3b (solid-gray line) and numerical estimations are summarized in Table 1. Comparison with theoretical values for  $\Delta G_{NU}$ ,

$x_F^\dagger$  and  $x_U^\dagger$  (provided in Table 2) reveals discrepancies. In the best case the relative error obtained for  $\Delta G_{NU}$  is approximately 20% for molecule HC.

Table 1: **Fit of the experimental kinetic rates for HN, HC and HB to the BE model.** The logarithm of the experimental kinetic rates plotted in Fig. 3b were fitted to Eqs. (1) and (2) over the whole force range to get estimations for  $k_m$ ,  $\Delta G_{FU}$ ,  $x_F^\dagger$ ,  $x_U^\dagger$  and  $f_c = \Delta G_{FU}/(x_F^\dagger + x_U^\dagger)$ . Error bars are calculated using error propagation of standard statistical errors from the fit. Systematic errors due to imperfect instrumental calibration are not included

Hairpin	$k_m$ (s <sup>-1</sup> )	$\Delta G_{FU}$ ( $k_B T$ )	$x_F^\dagger$ (nm)	$x_U^\dagger$ (nm)	$f_c$ (pN)	$\mu_c$ (ad.)
HN	$(2.6 \pm 0.5) \times 10^{-21}$	$76 \pm 2$	$10.5 \pm 0.3$	$8.6 \pm 0.3$	$16.3 \pm 0.7$	$0.10 \pm 0.06$
HC	$(1.8 \pm 0.5) \times 10^{-29}$	$90 \pm 3$	$15.6 \pm 0.7$	$6.5 \pm 0.2$	$16.7 \pm 0.7$	$0.41 \pm 0.07$
HB	$(2.8 \pm 0.6) \times 10^{-17}$	$68 \pm 2$	$9.5 \pm 0.3$	$10.2 \pm 0.5$	$14.0 \pm 0.5$	$-0.04 \pm 0.05$

Table 2: **Predicted parameters for BE model of HN, HC and HB.** Theoretical values for hairpins HN, HC and HB were obtained using the nearest-neighbor model by including the proper elastic contributions (see main text) and averaging the unified oligonucleotide set of parameters and unzipping predictions. Error bars are standard statistical errors. Statistical errors for fragilities are too small and they are not shown. Systematic errors due to imperfect instrumental calibration are not included.

Hairpin	$\Delta G_{FU}$ ( $k_B T$ )	$x_F^\dagger$ (nm)	$x_U^\dagger$ (nm)	$f_c$ (pN)	$\mu_c$ (ad.)
HN	$111 \pm 3$	$13.55 \pm 0.05$	$15.4 \pm 0.1$	$15.7 \pm 0.3$	0.00
HC	$118 \pm 4$	$24.05 \pm 0.05$	$5.5 \pm 0.1$	$16.3 \pm 0.5$	0.76
HB	$94 \pm 2$	$7.20 \pm 0.05$	$21.5 \pm 0.1$	$13.4 \pm 0.2$	-0.47

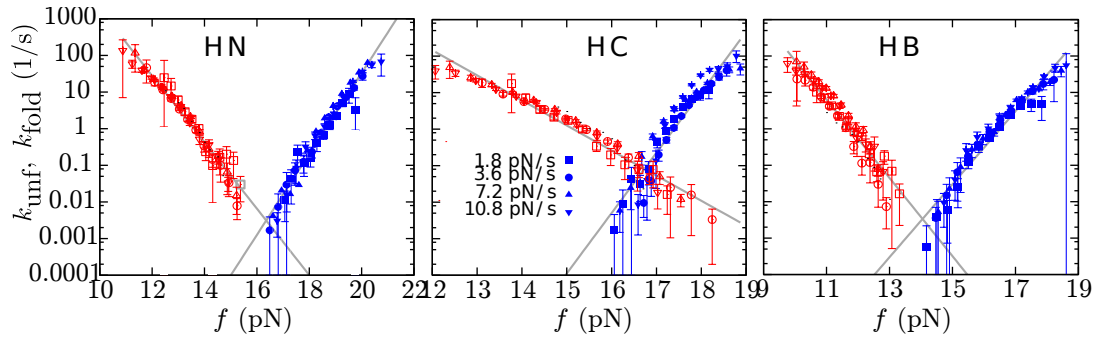


Figure 3: **Bell Evans model and kinetic rates for hairpins HN, HC and HB.** Kinetic rates of unfolding  $k_{\text{unf}}(f)$  (blue-solid symbols) and folding  $k_{\text{fold}}(f)$  (red-empty symbols) measured from pulling experiments performed at different loading rates, and fits to the BE model performed along the whole range of measured forces (solid-gray line) for the three hairpins HN, HC and HB.

### S3. Dudko-Hummer-Szabo model

According to the Dudko-Hummer-Szabo (DHS) model, the unfolding kinetic rates read as:

$$k_{\text{unf}}(f) = k_0 \left(1 - \gamma \frac{f x_F^\ddagger}{B}\right)^{1/\gamma-1} \exp \left\{ \frac{B}{k_B T} \left[1 - \left(1 - \gamma \frac{f x_F^\ddagger}{B}\right)^{1/\gamma}\right] \right\}. \quad (3)$$

Here,  $B$  is the kinetic barrier,  $k_0$  is the attempt frequency at zero force ( $k_0 \exp(-B/k_B T)$  being the unfolding kinetic rate at zero force),  $x_F^\ddagger$  is the relative distance between state F and the TS, and  $\nu = 1/2$  or  $\nu = 2/3$  is related to the shape of the unperturbed molecular free energy landscape. In what follows, we set  $\nu = 1/2$ .

In Fig. 4 and table 3 we show the results from the fit. It can be seen that even though the fragility dependence is captured ( $x_F^\ddagger(\text{HC}) > x_F^\ddagger(\text{HN}) > x_F^\ddagger(\text{HB})$ ), the numerical value obtained for  $x_F^\ddagger$  does not agree with the theoretical predictions (Table 2).

Table 3: **Fit of the experimental unfolding kinetic rates for HN, HC and HB to the DHS model** ( $\gamma = 1/2$ ). The experimental unfolding kinetic rates for HN, HC and HB were fitted to Eq. (3) over the whole force range to get estimations for  $k_0$ ,  $x_F^\ddagger$ , and  $B$ . Error bars are calculated from the fit.

Hairpin	$k_0$ (1/s)	$x_F^\ddagger$ (nm)	$B$ ( $k_B T$ )
HN	$\exp(-140 \pm 20)$	$50 \pm 7$	$146 \pm 16$
HC	$\exp(-340 \pm 60)$	$145 \pm 25$	$347 \pm 56$
HB	$\exp(-110 \pm 10)$	$44 \pm 5$	$114 \pm 10$

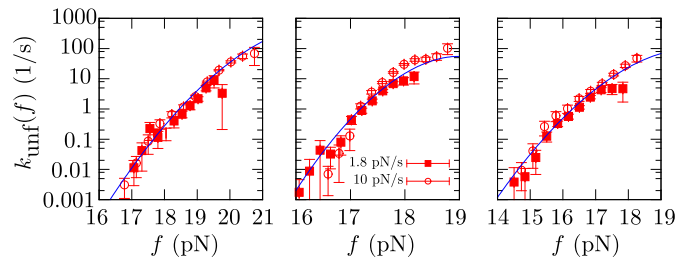


Figure 4: **Dudko-Hummer-Szabo model and kinetic rates for hairpins HN, HC and HB.** Kinetic rates of unfolding  $k_{\text{unf}}(f)$  (blue-solid symbols) measured from pulling experiments performed at different loading rates, and fits to the DHS model performed along the whole range of measured forces (solid-gray line) for the three hairpins HN, HC and HB (from left to right).

## S4. Continuous Effective Barrier Analysis

Based on Eq. (4a) the following  $\chi^2_{\text{unf}}$  function can be defined:

$$\chi^2_{\text{unf}} = \sum_{i=1}^{N_u} \left[ \frac{B_{NU}^{\text{th}}(f_i)}{k_B T} - (\log k_0^{NU} - \log k_{\text{unf}}(f_i)) \right]^2, \quad (4)$$

where  $N_u$  is the total number of points for the experimental unfolding kinetic rate,  $\log k_{\text{unf}}(f_i)$  is the experimentally measured logarithm of the unfolding kinetic rate at force  $f_i$  ( $i = 1, \dots, N_u$ ), and  $B_{NU}^{\text{th}}(f_i)$  is the theoretical value of the height of the kinetic barrier obtained at  $f_i$ , measured using Eq. (5) in the main text.

Similarly, based on Eq. (4b) the following  $\chi^2_{\text{fold}}$  function can be defined:

$$\chi^2_{\text{fold}} = \sum_{i=1}^{N_f} \left[ \frac{B_{NU}^{\text{th}}(f_i)}{k_B T} - \left( \log k_0^{NU} + \frac{\Delta G_{NU}(f_i)}{k_B T} - \log k_{\text{fold}}(f_i) \right) \right]^2, \quad (5)$$

where  $N_f$  is the total number of points for the experimental folding kinetic rate,  $\log k_{\text{fold}}(f_i)$  is the experimentally measured logarithm of the folding kinetic rate at force  $f_i$  ( $i = 1, \dots, N_f$ ),  $B_{NU}^{\text{th}}(f_i)$  is the theoretical value of the height of the kinetic barrier obtained at  $f_i$ , and  $\Delta G_{NU}(f_i) = \Delta G_U(f_i) - \Delta G_N(f_i)$  is the free-energy difference between states  $U$  and  $N$  at  $f_i$  (Eq. 1).

The total  $\chi^2$  function is defined as:

$$\chi^2 = \chi^2_{\text{unf}} + \chi^2_{\text{fold}}. \quad (6)$$

The best match between the experimental and the theoretical profile of the force-dependent kinetic barrier is given by the values of  $\log k_0^{NU}$  and  $\Delta G_{NU}^0$  that minimize this  $\chi^2$  function. From the derivatives of  $\chi^2$  as a function of  $\log k_0^{NU}$  and  $\Delta G_{NU}^0$  it can be shown that best

estimators for both magnitudes are:

$$\log k_0^{NU} = \frac{1}{N_u} \sum_{i=1}^{N_u} \left[ \frac{B_{BU}^{\text{th}}(f_i)}{k_B T} + \log k_{\text{unf}}(f_i) \right] \quad (7)$$

$$\begin{aligned} \Delta G_{NU}^0 = \frac{1}{N_f} \sum_{i=1}^{N_f} \left[ B_{NU}^{\text{th}}(f_i) + \int_0^{f_i} x_{n=N}(f') df' - \int_0^{f_i} x_d(f') df' \right. \\ \left. + k_B T \log k_{\text{fold}}(f_i) \right] - k_B T \log k_0. \end{aligned} \quad (8)$$

If the elastic properties of the single-stranded nucleic acid are unknown, the  $\chi^2$  function can also be minimized for the persistence length  $P$ . Hence, the trio of values of  $P$ ,  $\log k_0^{NU}$  and  $\Delta G_{NU}^0$  that satisfy:

$$\frac{\partial \chi^2}{\partial P} = 0, \quad \frac{\partial \chi^2}{\partial \log k_0^{NU}} = 0, \quad \frac{\partial \chi^2}{\partial \Delta G_{NU}^0} = 0, \quad (9a,b,c)$$

give the best match between the theoretical and the experimental profile of the kinetic barrier when elastic properties are unknown.

The solution to the set of equations (9a,b,c) can be found numerically. The methodology followed is:

1. Select a range of reasonable values for the persistence length  $P$ .
2. For each value of  $P$ , compute  $\Delta G_{NU}^0$  and  $\log k_0^{NU}$  according to Eq. (7).
3. For each trio of values of  $P$ ,  $\Delta G_{NU}^0$  and  $\log k_0^{NU}$ , calculate the numerical value of the  $\chi^2$  function (Eq. 6).
4. Find the trio of values  $P$ ,  $\Delta G_{NU}^0$  and  $\log k_0^{NU}$  such that  $\chi^2$  has an absolute minimum.

In Fig. 5, the value of  $\chi^2$  as a function  $P$  for hairpins HN, HC and HB is shown. The result depends on the set of basepair free energies used to calculate  $B_{NU}^{\text{th}}(f)$  (unified oligonucleotide dataset versus unzipping predictions). Estimations for  $k_0$ ,  $\Delta G_{NU}^0$  and  $P$  are the average over the results obtained using the two different sets of basepair free energies.



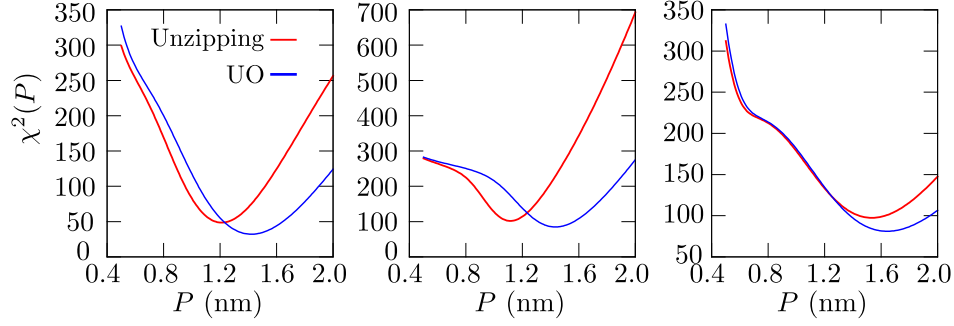


Figure 5:  $\chi^2$  **versus persistence length**  $P$ . Red-solid line was obtained by using the UO set of base-pair free energies from<sup>1</sup> for the evaluation of  $B^{\text{th}}(f)$  and blue-dashed line was obtained by using the unzipping predictions from.<sup>2</sup>

## References

- (1) SantaLucia, J. A unified view of polymer, dumbbell, and oligonucleotide DNA nearest-neighbor thermodynamics. *Proc. Natl. Acad. Sci. USA* **1998** 95, 1460–1465.
- (2) Huguet, J. M.; Bizarro, C. V.; Forns, N.; Smith, S. B.; Bustamante, C.; Ritort, F. Single-molecule derivation of salt dependent base-pair free energies in DNA. *Proc. Natl. Acad. Sci. USA* **2010**, 107, 15431–15436.